Ganpat University
॥ विद्यया समाजोत्कर्षः ॥

University Journal of Research
ISSN (Online) 2455-1724

Mathematical analysis of MHD Casson fluid flow through porous medium with Hall Current and Thermo-diffusion

Snehal D Patel [a*], Dr. Harshad R Patel [a]

[a]*Ganpat University- U. V. Patel College of Engineering, Kherva, Gujarat, India.*

Abstract

This research looks into the effect of thermo-diffusion and Hall Current effects on MHD flow of Casson fluid past an exponentially accelerated vertical plate in rotating system. The flow confined in porous medium. Similarity transformation converts the momentum, energy, and concentration PDEs into ODEs. The analytical expression of said problems is obtained using the Laplace transform technique. For better understanding of the problems, approximation solution is defined and presented graphically for different physical parameter. From graphical representation, we observe that Hall current tends to improve motion of the flow field in both directions x' and z' throughout the flow field. It is also concluded that the rotation parameter K tends to reduce primary velocity whereas rotation parameter K tends to improve secondary velocity.

Keywords: *Magnetohydrodynamics; Unsteady Casson fluid flow; Porous medium; Thermo-diffusion; Chemical reaction.*

Nomenclature

B_0 Uniform magnetic field
C′ Concentration
D_M Mass diffusion coefficient
D_T Thermal diffusion coefficient
Gr Grashof No. (Thermal)
Gm Grashof number (Mass)
k_1 Permeability parameter
Sc Schmidt No.
k_2' Chemical reaction
Pr Prandtl number
t′ Time
q_r Radiative heat flux
∅ Porosity of the porous medium
σ Electrical conductivity
Sc Schmidt number
Nr Thermal Radiation
θ Dimensionless fluid temperature
u primary velocity in x direction
w secondary velocity in x direction
C Concentration (Dimensionless)
M Magnetic field parameter
Kr Reaction Parameter
m Hall current
k rotation parameter
U_0 uniform velocity of the plate
γ Casson fluid parameter
Ω uniform angular velocity
t Dimensionless time
ω phase angle

INTRODUCTION

Magnetohydrodynamics (MHD) studies how magnetic fields interact with electrically conducting fluids. MHD fluids include electrolytes, plasmas, liquid metals, and saltwater. Hannes Alfven founded MHD and won the 1970 Nobel Prize in physics for it. MHD has various practical uses in a variety of fields, including astronomy, engineering, geophysics, medicine, and the health sciences. Due of its technical and industrial implications, electrically conductive fluids have attracted numerous researchers. Early researchers [1]– [5] made crucial contributions that made this area so significant for the last two decades. Casson fluid is often considered to be the superior option among non-Newtonian fluids. Because the Casson fluid acts like an elastic solid, the constitutive

*Corresponding Author
E-mail address: sdp01@ganpatuniversity.ac.in

equation includes a yield shear stress in its solution. For examples blood, tomato soup, jelly, shampoo, ketchup, toothpaste etc. Initially Casson fluid is a good research topic since it has many engineering and technological applications. Edwin Hall [3] found Hall current in 1879. Hall current is guaranteed to be present whenever an electric field is placed in proximity to a magnetic conductor. Hall current has several applications, including magnetometers, fuel gauges in vehicles, power generators, and many more. Radiation is electromagnetic heat transmission. The radiation plays a crucial role in many high-temperature mechanical procedures, such as nuclear reactors, propulsion equipment and gas turbines. The consequence of chemical reaction can be considerable in situations that include the exchange of thermal energy and mass. So, many researchers examined chemical reaction in MHD flow issues. Using a semi-infinite vertical plate as a channel for mass transfer in a magnetohydrodynamic flow, E. M. Aboeldahab et al. [4] analysed the Hall current influence on this type of flow. Sharma [5] studied effects of heat transfer on MHD flow. O. D. Makinde [6] studied MHD flow with radiation including mass transfer. An exact solution for Casson fluid flow with stretching surface was found by Mukhopadhyay et al. [7]. Researchers led by Sandeep and his colleagues investigated the impact of magnetic fields. Hall current and thermos-diffusion effects on magnetohydrodynamics flow through an accelerated vertical plate via a porous material were examined by Sarma et al. [8]. Using perturbation solutions, Sulochana et al. [9] analysed the dynamics of a Casson liquid moving across a plate subject to Hall effects in an unstable MHD condition. Harshad Patel [10] and Prasad et al. [11] constructed the model of double diffusion effects on MHD Casson fluid flow in porous media. For the effects of the Hall and slip on MHD rotational flow in porous media, Veera Krishna et al. [12] designed a mathematical model. Further he [13] studied the effects of a constant transverse magnetic field, heat absorption, and unsteady MHD flow of nanofluids. Xiang-Li et al. [14] studied the constant thermal source and sink and viscous dissipation in the MHD flow of Casson nanoparticles towards a porous stretchy sheet. Reddy et al. [15] discussed computational study of mixed convection MHD flow to understand thermo-diffusion and heat generation effects. Patel and Patel [16] discussed heat and mass transfer effects on MHD micropolar fluid. Further they [17] extended their work for unsteady MHD flow. Hall effect and Cross-diffusion effects were discussed by Mkhatshwa et al. [18] on natural convection MHD flow of nanofluid. Hall current and heat generation effects were investigated by Sahoo et al. [19] on non-Darcy Casson nano fluid flow.

NOVELTY OF THE PROBLEM

Purpose of this paper to investigated exact solution of thermo-diffusion and Hall effects on MHD flow of chemically reactive Casson fluid past an exponentially accelerated vertical plate through uniform porous medium in a rotating system. The governing dimensionless equations with imposed initial boundary are solved using Laplace transform technique and obtained analytical results. For importance of different physical parameter effects on flow, the numerical results are obtained and represent through a graph. Such study may find application in fire dynamics in insulations and geothermal energy systems etc.

MATHEMATICAL FORMULATION

In Figure.1, the x' as along the plate, y' as normal to it and z' as the perpendicular to $x'y'$. The plate and fluid are rotate with Ω (angular velocity) about $y'-$ axis. Initially, T'_∞ and C'_∞ is considered temperature and concentration at $t' \leq 0$ respectively whereas, T'_w and $C'_\infty + (C'_w - C'_\infty)\, t'/t_0$ is considered temperature and concentration at $t' > 0$ respectively after that the concentration C'_w is maintained.

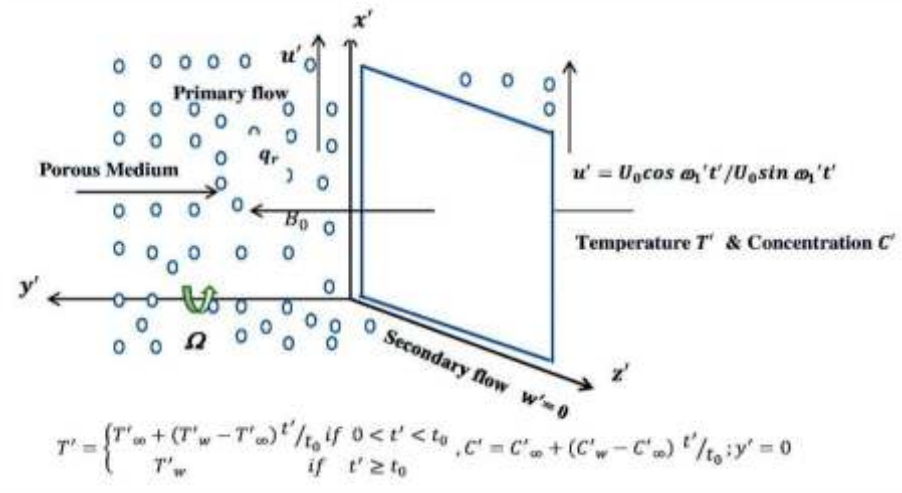

Figure 1: Physical sketch of the problem

Under above assumptions and Boussinesq's approximation, governing momentum, energy and concentration equations can be written as,

$$\rho\frac{\partial u'}{\partial t'} + 2\Omega w' = \mu B\left(1+\frac{1}{\gamma}\right)\frac{\partial^2 u'}{\partial y'^2} - \frac{\sigma {B_0}^2}{(1+m^2)}(u' + mw') - \frac{\mu B}{k_1'}u' + g\rho\beta'_T(T' - T'_\infty) + g\rho\beta'_C(C' - C'_\infty) \quad (1)$$

$$\rho\frac{\partial w'}{\partial t'} - 2\Omega u' = \mu B\left(1+\frac{1}{\gamma}\right)\frac{\partial^2 w'}{\partial y'^2} - \frac{\sigma {B_0}^2}{(1+m^2)}(mu' - w') - \frac{\mu B}{k_1'}u' \quad (2)$$

$$\frac{\partial T'}{\partial t'} = \frac{k}{\rho c_p}\frac{\partial^2 T'}{\partial y'^2} \quad (3)$$

$$\frac{\partial C'}{\partial t'} = D_M\frac{\partial^2 C'}{\partial y'^2} + D_T\frac{\partial^2 T'}{\partial y'^2} - k_2'(C' - C'_\infty) \quad (4)$$

With initial and boundary condition

$$u' = 0,\ w' = 0 \quad T' = T'_\infty,\ C' = C'_\infty;\ as\ \ y' \geq 0\ and\ \ t' \leq 0$$

$$u' = U_0 e^{at'},\ w' = 0\ , T' = T'_w\ ,$$

$$C' = C'_\infty + (C'_w - C'_\infty)\ {t'}/{t_0};\ \ t' \geq 0\ and\ y' = 0,$$

$$u' \to 0, T' \to T'_\infty, C' \to C'_\infty;\ as\ \ y' \to \infty\ and\ t' \geq 0 \quad (5)$$

The dimensionless parameter is defined as,

$$y = \frac{y'}{U_0 t_0},\ u = \frac{u'}{U_0},\ t = \frac{t'}{t_0},\ \theta = \frac{(T'-T'_\infty)}{(T'_w - T'_\infty)},\ C = \frac{(C'-C'_\infty)}{(C'_w - C'_\infty)}$$

The dimensionless form of equations (1) to (5) can be written as,

$$\frac{\partial u}{\partial t} + 2k^2 w = \left(1+\frac{1}{\gamma}\right)\frac{\partial^2 u}{\partial y^2} - \frac{M^2}{1+m^2}(u + mw) - \frac{1}{k_1}u + G_r\theta + G_m C \quad (6)$$

$$\frac{\partial w}{\partial t} - 2k^2 u = \left(1+\frac{1}{\gamma}\right)\frac{\partial^2 v}{\partial y^2} + \frac{M^2}{1+m^2}(mu - w) - \frac{1}{k_1}w \quad (7)$$

$$\frac{\partial \theta}{\partial t} = \frac{1}{Pr}\frac{\partial^2 \theta}{\partial y^2} \quad (8)$$

$$\frac{\partial C}{\partial t} = \frac{1}{s_c}\frac{\partial^2 C}{\partial y^2} + Sr\frac{\partial^2 \theta}{\partial y^2} - krC \quad (9)$$

With initial and boundary condition

$$u = w = \theta = C = 0\ , \qquad y \geq 0, t \leq 0$$

$$u = e^{at}, w = 0\ ,\ \theta = 1,\ C = t\ at\ \ y = 0,\ \ t > 0$$

$$u \to 0, w \to 0, \theta \to 0, C \to 0 \quad at\ \ y \to \infty,\ \ t > 0 \quad (10)$$

In above non-dimensional equations (6-7) combined using the substitution $F = u + iw$

$$\frac{\partial F}{\partial t} + \left(\frac{M^2(1-im)}{1+m^2} + \frac{1}{k_1} - 2ik^2\right)F = \left(1+\frac{1}{\gamma}\right)\frac{\partial^2 F}{\partial y^2} + G_r\theta + G_m C \quad (11)$$

$$\frac{\partial \theta}{\partial t} = \frac{1}{Pr}\frac{\partial^2 \theta}{\partial y^2} \quad (12)$$

$$\frac{\partial C}{\partial t} = \frac{1}{s_c}\frac{\partial^2 C}{\partial y^2} + Sr\frac{\partial^2 \theta}{\partial y^2} - krC \quad (13)$$

With initial and boundary condition

$$F = \theta = C = 0\ , \qquad y \geq 0, t \leq 0$$

$$F = e^{at}\ ,\ \theta = 1, C = t\ at\ \ y = 0,\ \ t > 0$$

$$F \to 0, \theta \to 0, C \to 0 \quad at \ \ y \to \infty, \ \ t > 0 \tag{14}$$

Where, $Gr = \frac{\nu g \beta'_T (T'_w - T'_\infty)}{U_0^3}, Gm = \frac{\nu g \beta'_C (C'_w - C'_\infty)}{U_0^3}$, $M = \frac{\sigma B_0^2 \nu}{\rho U_0^2}$, $P_r = \frac{\rho \nu C_p}{k}$ $Sc = \frac{\nu}{D_M}, Kr = \frac{\nu k_2'}{U_0^2}$, $k_1 = \frac{\nu \emptyset}{k_1'}$

SOLUTION OF THE PROBLEM

The results are obtained through Laplace transform technique. So, Taking LT of equations (11) to (13) with I.C. and B.C. (14).

$$\bar{\theta}(y, s) = \frac{1}{s} e^{-\sqrt{P_r S}\, y} = F_{12}(y, s) \tag{15}$$

$$\bar{C}(y, s) = F_{13}(y, s) - a_4 F_{15}(y, s) + a_4 F_{11}(y, s) \tag{16}$$

$$\bar{F} = G_1(y, s) + G_2(y, s) + G_3(y, s) \tag{17}$$

Where,

$$G_1 = F_1(y, s) + a_{23} F_2(y, s) + a_{15} F_3(y, s) - a_{16} F_4 + a_{24} F_5 + a_{25} F_6 - a_{22} F_7 \tag{18}$$

$$G_2 = a_{15} F_8 - a_{15} F_9 + a_{22} F_{10} + a_{21} F_{11} \tag{19}$$

$$G_3 = a_{18} F_{12} + a_{16} F_{13} + a_{24} F_{14} - a_{19} F_{15} \tag{20}$$

$$F_1 = \frac{1}{s-a} \ e^{-\sqrt{\frac{s+a_0}{a_1}}\, y} \tag{21}$$

$$F_2 = \frac{1}{s} \ e^{-\sqrt{\frac{s+a_0}{a_1}}\, y} \tag{22}$$

$$F_3 = \frac{1}{s-a_6} \ e^{-\sqrt{\frac{s+a_0}{a_1}}\, y} \tag{23}$$

$$F_4 = \frac{1}{s^2} \ e^{-\sqrt{\frac{s+a_0}{a_1}}\, y} \tag{24}$$

$$F_5 = \frac{1}{s+a_{10}} \ e^{-\sqrt{\frac{s+a_0}{a_1}}\, y} \tag{25}$$

$$F_6 = \frac{1}{s-a_3} \ e^{-\sqrt{\frac{s+a_0}{a_1}}\, y} \tag{26}$$

$$F_7 = \frac{1}{s-a_{13}} \ e^{-\sqrt{\frac{s+a_0}{a_1}}\, y} \tag{27}$$

$$F_8 = \frac{1}{s} \ e^{-\sqrt{P_r S}\, y} \tag{28}$$

$$F_9 = \frac{1}{s-a_6} \ e^{-\sqrt{P_r S}\, y} \tag{29}$$

$$F_{10} = \frac{1}{s-a_3} \ e^{-\sqrt{P_r S}\, y} \tag{30}$$

$$F_{11} = \frac{1}{s-a_3} \ e^{-\sqrt{P_r S}\, y} \tag{31}$$

$$F_{12} = \frac{1}{s} \ e^{-\sqrt{S_c (S+K_r)}\, y} \tag{32}$$

$$F_{13} = \frac{1}{s^2} \ e^{-\sqrt{S_c (S+K_r)}\, y} \tag{33}$$

$$F_{14} = \frac{1}{s+a_{10}} \ e^{-\sqrt{S_c (S+K_r}\, y} \tag{34}$$

$$F_{15} = \frac{1}{s-a_3} \ e^{-\sqrt{S_c (S+K_r)}\, y} \tag{35}$$

Taking inverse Laplace transform technique of equations (15) to (35), we get analytic results of velocity, temperature and concentration profiles.

$$\theta(y,t) = f_{12} \tag{36}$$

$$\mathrm{C}(y,t) = f_{13} - a_4 f_{15} + a_4\, f_{11} \tag{37}$$

$$F(y\,,t) = g_1 + g_2 + g_3 \tag{38}$$

Where,

$$g_1(y,t) = f_1 + a_{23}f_2 + a_{15}f_3 - a_{16}f_4 + a_{24}f_5 + a_{25}f_6 - a_{22}f_7) \tag{39}$$

$$g_2(y,t) = a_{15}f_8 - a_{15}f_9 + a_{22}f_{10} + a_{21}f_{11} \tag{40}$$

$$g_3(y,t) = a_{18}f_{12} + a_{16}f_{13} + a_{24}f_{14} - a_{19}f_{15} \tag{41}$$

$$f_1(y,t) = L^{-1}\left(\frac{1}{s-a}\ e^{-\sqrt{\frac{s+a_0}{a_1}}y}\right) = \frac{e^{-a\,t}}{2}\left[e^{-y\sqrt{\frac{1}{a_1}(a_0-a)}}\ erfc\ \left(\frac{y}{2\sqrt{a_1\,t}} - \sqrt{(a_0-a)t}\right) + e^{y\sqrt{\frac{1}{a_1}(a_0-a)}}\ erfc\ \left(\frac{y}{2\sqrt{a_1\,t}} + \sqrt{(a_0-a)t}\right)\right] \tag{42}$$

$$f_2(y,t) = L^{-1}\left(\frac{1}{s}\ e^{-\sqrt{\frac{s+a_0}{a_1}}y}\right) = \frac{1}{2}\left[e^{-y\sqrt{\frac{a_0}{a_1}}}\ erfc\ \left(\frac{y}{2\sqrt{a_1 t}} - \sqrt{a_0 t}\right) + e^{y\sqrt{\frac{a_0}{a_1}}}\ erfc\ \left(\frac{y}{2\sqrt{a_1 t}} + \sqrt{a_0 t}\right)\right] \tag{43}$$

$$f_3(y,t) = L^{-1}\left(\frac{1}{s-a_6}\ e^{-\sqrt{\frac{s+a_0}{a_1}}y}\right) = \frac{e^{-a_6\,t}}{2}\left[e^{-y\sqrt{\frac{1}{a_1}(a_0-a_6)}}\ erfc\ \left(\frac{y}{2\sqrt{a_1\,t}} - \sqrt{(a_0-a_6)t}\right) + e^{y\sqrt{\frac{1}{a_1}(a_0-a_6)}}\ erfc\ \left(\frac{y}{2\sqrt{a_1\,t}} + \sqrt{(a_0-a_6)t}\right)\right] \tag{44}$$

$$f_4(y,t) = L^{-1}\left(\frac{1}{s^2}\ e^{-\sqrt{\frac{s+a_0}{a_1}}y}\right) = \frac{1}{2}\left[\left(t - \frac{y}{2\sqrt{a_0 a_1}}\right)e^{-y\sqrt{\frac{a_0}{a_1}}}\ erfc\ \left(\frac{y}{2\sqrt{a_0 a_1}} - \sqrt{\sqrt{a_0}t}\right) + \left(t + \frac{y}{2\sqrt{a_0 a_1}}\right)e^{y\sqrt{\frac{a_0}{a_1}}}\ erfc\ \left(\frac{y}{2\sqrt{a_1 t}} + \sqrt{a_0 t}\right)\right] \tag{45}$$

$$f_5(y,t) = L^{-1}\left(\frac{1}{s+a_{10}}\ e^{-\sqrt{\frac{s+a_0}{a_1}}y}\right) = \frac{e^{a_{10}\,t}}{2}\left[e^{-y\sqrt{\frac{1}{a_1}(a_0+a_{10})}}\ erfc\ \left(\frac{y}{2\sqrt{a_1\,t}} - \sqrt{(a_0+a_{10})t}\right) + e^{y\sqrt{\frac{1}{a_1}(a_0+a_{10})}}\ erfc\ \left(\frac{y}{2\sqrt{a_1\,t}} + \sqrt{(a_0+a_{10})t}\right)\right] \tag{46}$$

$$f_6(y,t) = L^{-1}\left(\frac{1}{s-a_3}\ e^{-\sqrt{\frac{s+a_0}{a_1}}y}\right) = \frac{e^{-a_3\,t}}{2}\left[e^{-y\sqrt{\frac{1}{a_1}(a_0-a_3)}}\ erfc\ \left(\frac{y}{2\sqrt{a_1\,t}} - \sqrt{(a_0-a_3)t}\right) + e^{y\sqrt{\frac{1}{a_1}(a_0-a_3)}}\ erfc\ \left(\frac{y}{2\sqrt{a_1\,t}} + \sqrt{(a_0-a_3)t}\right)\right] \tag{47}$$

$$f_7(y,t) = L^{-1}\left(\frac{1}{s-a_{13}}\ e^{-\sqrt{\frac{s+a_0}{a_1}}y}\right) = \frac{e^{-a_{13}\,t}}{2}\left[e^{-y\sqrt{\frac{1}{a_1}(a_0-a_{13})}}\ erfc\ \left(\frac{y}{2\sqrt{a_1\,t}} - \sqrt{(a_0-a_{13})t}\right) + e^{y\sqrt{\frac{1}{a_1}(a_0-a_{13})}}\ erfc\ \left(\frac{y}{2\sqrt{a_1\,t}} + \sqrt{(a_0-a_{13})t}\right)\right] \tag{48}$$

$$f_8(y,t) = \frac{1}{s}\ e^{-\sqrt{P_r\,S}\,y} = erfc\left(\frac{1}{2}\sqrt{\frac{Pr}{t}}\ y\right) \tag{49}$$

$$f_9(y,t) = \frac{1}{s-a_6}\ e^{-\sqrt{P_r\,S}\,y} = \frac{e^{a_6\,t}}{2}\left[e^{-y\sqrt{P_r\,a_6}}\ erfc\ \left(\frac{y\sqrt{P_r}}{2\sqrt{t}} - \sqrt{a_6 t}\right) + e^{y\sqrt{P_r\,a_6}}\ erfc\ \left(\frac{y\sqrt{P_r}}{2\sqrt{t}} + \sqrt{a_6 t}\right)\right] \tag{50}$$

$$f_{10}(y,t) = \frac{1}{s-a_{13}}\ e^{-\sqrt{P_r\, S}\, y} = \frac{e^{a_{13}\, t}}{2}\left[e^{-y\sqrt{P_r\, a_{13}}}\ erfc\ \left(\frac{y\sqrt{P_r}}{2\sqrt{t}} - \sqrt{a_{13}t}\right) + e^{y\sqrt{P_r\, a_{13}}}\ erfc\ \left(\frac{y\sqrt{P_r}}{2\sqrt{t}} + \sqrt{a_{13}t}\right)\right] \quad (51)$$

$$f_{11}(y,t) = \frac{1}{s-a_3}\ e^{-\sqrt{P_r\, S}\, y} = \frac{e^{a_3\, t}}{2}\left[e^{-y\sqrt{P_r\, a_3}}\ erfc\ \left(\frac{y\sqrt{P_r}}{2\sqrt{t}} - \sqrt{a_3 t}\right) + e^{y\sqrt{P_r\, a_3}}\ erfc\ \left(\frac{y\sqrt{P_r}}{2\sqrt{t}} + \sqrt{a_3 t}\right)\right] \quad (52)$$

$$f_{12}(y,t) = L^{-1}\left(\frac{1}{s}\ e^{-\sqrt{S_c(\,S+K_r)}\, y}\right) = \frac{1}{2}\left[e^{-y\sqrt{Sc.\ Kr}}\ erfc\ \left(\frac{y}{2\sqrt{\frac{t}{Sc}}} - \sqrt{Kr.t}\right) + e^{y\sqrt{Sc.\ Kr}}\ erfc\ \left(\frac{y}{2\sqrt{\frac{t}{Sc}}} + \sqrt{Kr.t}\right)\right] \quad (53)$$

$$f_{13}(y,t) = L^{-1}\left(\frac{1}{s^2}\ e^{-\sqrt{S_c(\,S+K_r)}\, y}\right) = \frac{1}{2}\left[\left(t - \frac{y}{2\sqrt{\frac{Kr}{Sc}}}\right)e^{-y\sqrt{Sc.Kr}}\ erfc\ \left(\frac{y}{2\sqrt{\frac{Kr}{Sc}}} - \sqrt{Kr.t}\right) + \left(t + \frac{y}{2\sqrt{\frac{Kr}{Sc}}}\right)e^{y\sqrt{Sc.Kr}}\ erfc\ \left(\frac{y}{2\sqrt{\frac{t}{Sc}}} + \sqrt{Kr.t}\right)\right] \quad (54)$$

$$f_{14}(y,t) = L^{-1}\left(\frac{1}{s+a_{10}}\ e^{-\sqrt{S_c(\,S+K_r)}\, y}\right) = \frac{e^{a_{10}\, t}}{2}\left[e^{-y\sqrt{S_c(\,S+K_r)}}\ erfc\ \left(\frac{y}{2\sqrt{\frac{t}{Sc}}} - \sqrt{(Kr+a_{10})t}\right) + e^{y\sqrt{S_c(\,S+K_r)}}\ erfc\ \left(\frac{y}{2\sqrt{\frac{t}{Sc}}} + \sqrt{(Kr+a_{10})t}\right)\right] \quad (55)$$

$$f_{15}(y,t) = L^{-1}\left(\frac{1}{s-a_3}\ e^{-\sqrt{S_c(\,S+K_r)}\, y}\right) = \frac{e^{-a_3\, t}}{2}\left[e^{-y\sqrt{Sc(Kr-a_3)}}\ erfc\ \left(\frac{y}{2\sqrt{\frac{t}{Sc}}} - \sqrt{(Kr-a_3)t}\right) + e^{y\sqrt{Sc(Kr-a_3)}}\ erfc\ \left(\frac{y}{2\sqrt{\frac{t}{Sc}}} + \sqrt{(Kr-a_3)t}\right)\right] \quad (56)$$

RESULTS AND DISCUSSIONS

The understanding of physics, numerical solution is obtained with various values of parameter and presented through the Figures 2 to 7. We can see how Hall current m influences both the main and secondary fluid velocities in Figs. 2 and 3.

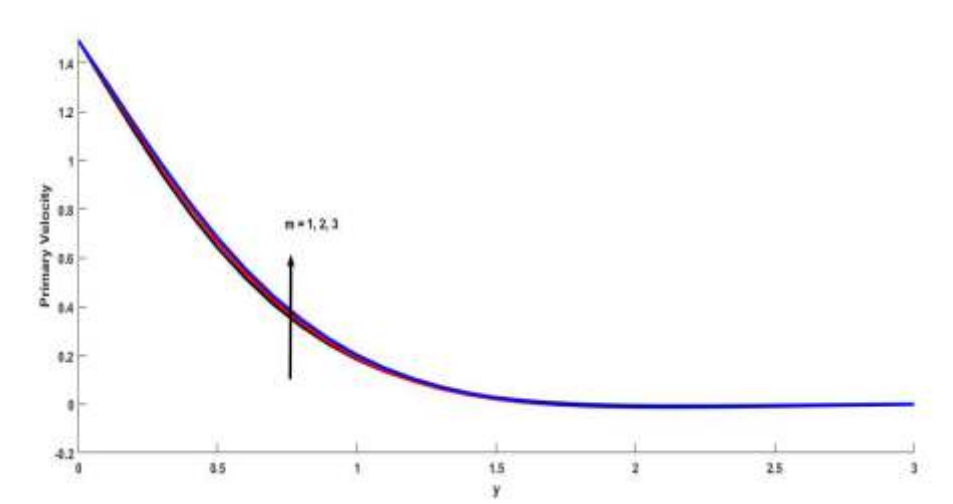

Figure 2: Primary velocity u for different values y and m.

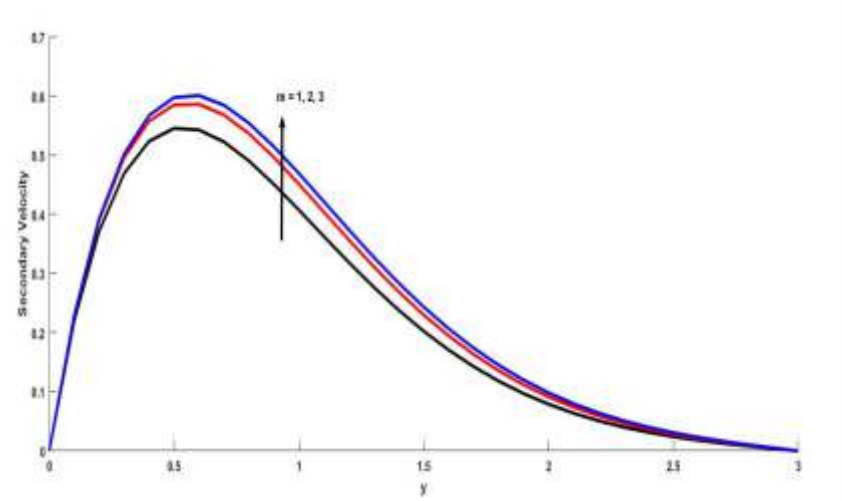

Fig. 3: Secondary velocity w for different values of y and m.

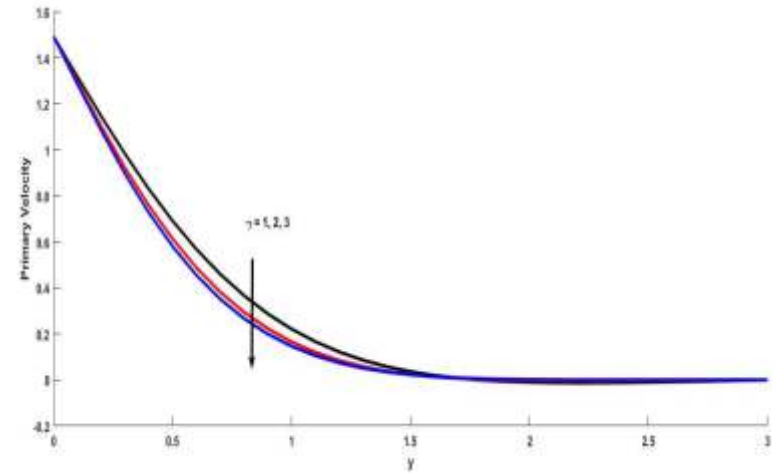

Fig. 4: Primary velocity u for different values of y and γ.

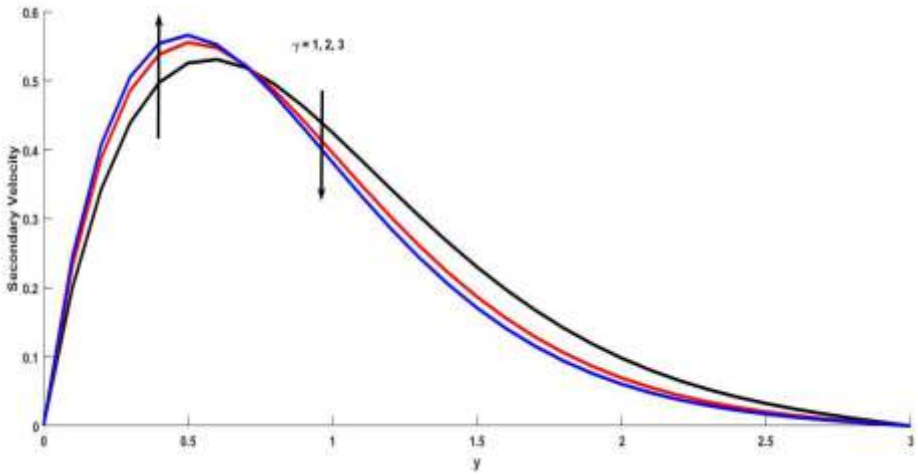

Fig. 5: Secondary velocity w for different values of y and γ.

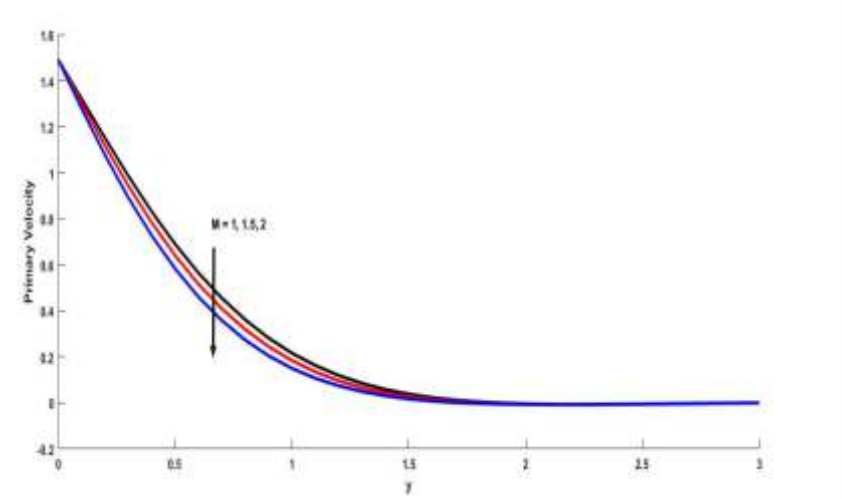

Fig. 6: Primary velocity u for different values of y and M.

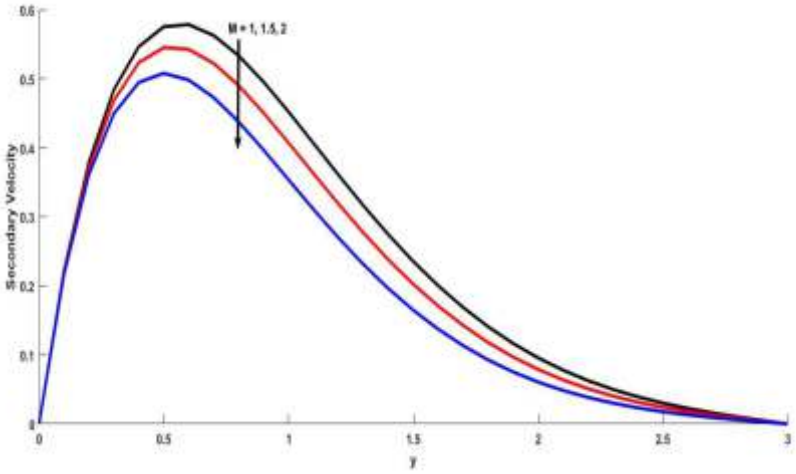

Fig.7: Secondary velocity w for different values of y and M.

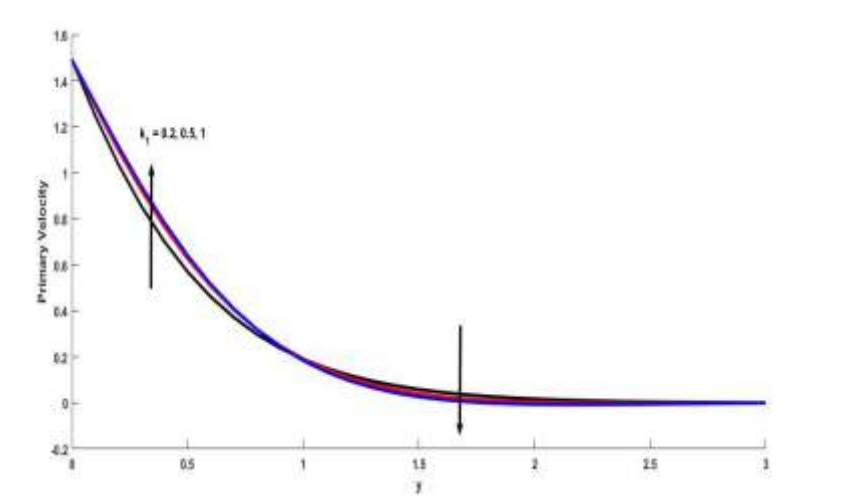

Fig. 8: Primary velocity u for different values of y and k_1.

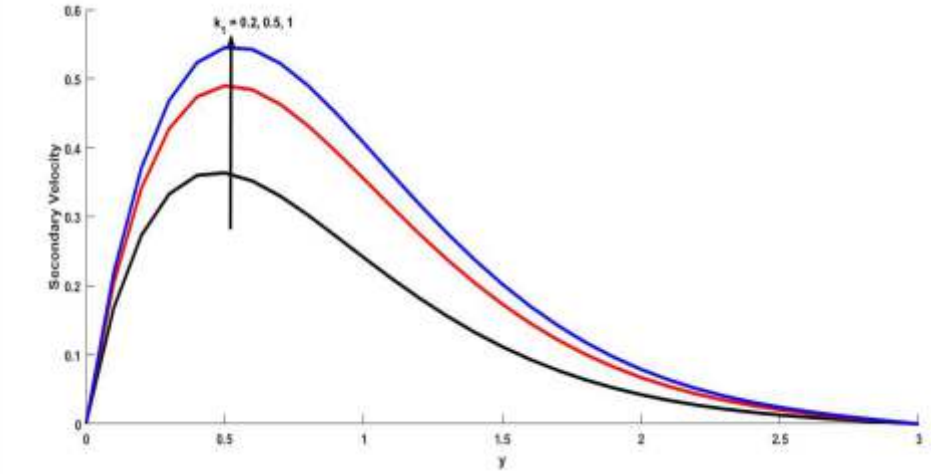

Fig. 9: Secondary velocity w for different values of y and k_1.

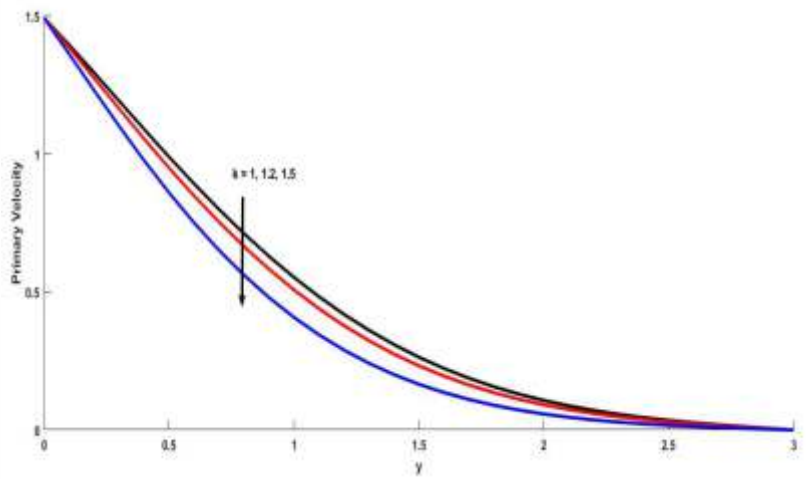

Fig.10: Primary velocity u for different values of y and K.

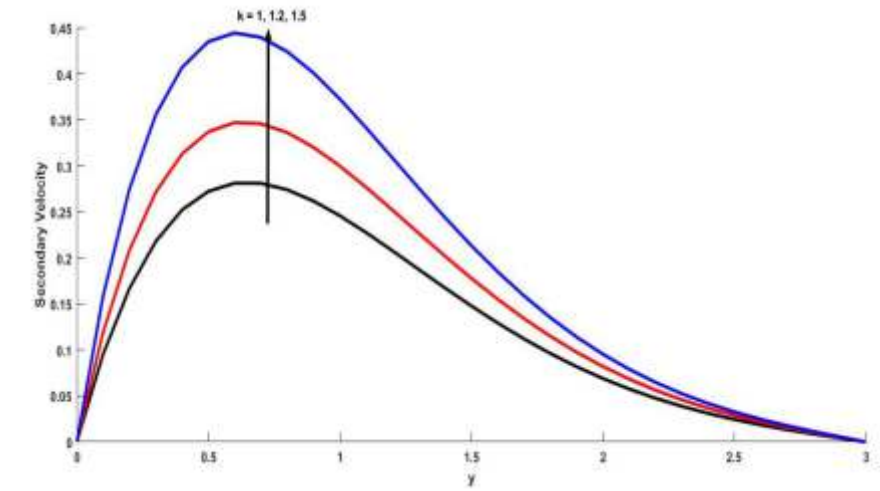

Fig. 11: Secondary velocity w for different values of y and K.

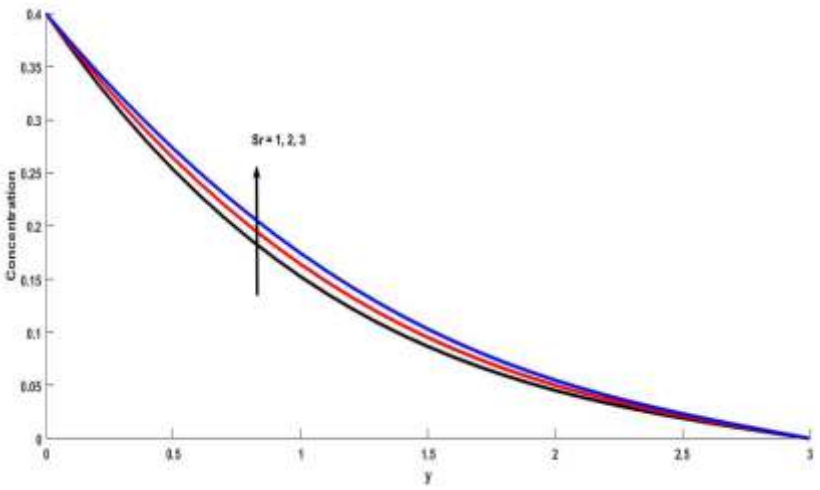

Fig. 12: Concentration C for different values of y and Sr.

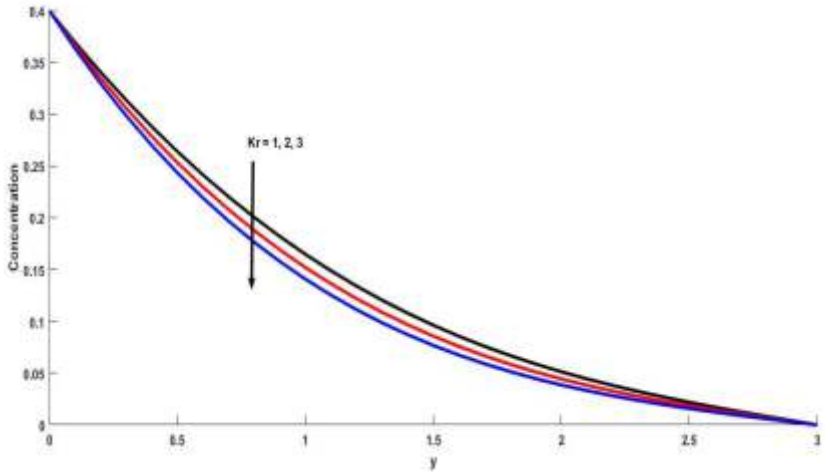

Fig. 13: Concentration C for different values of y and Kr.

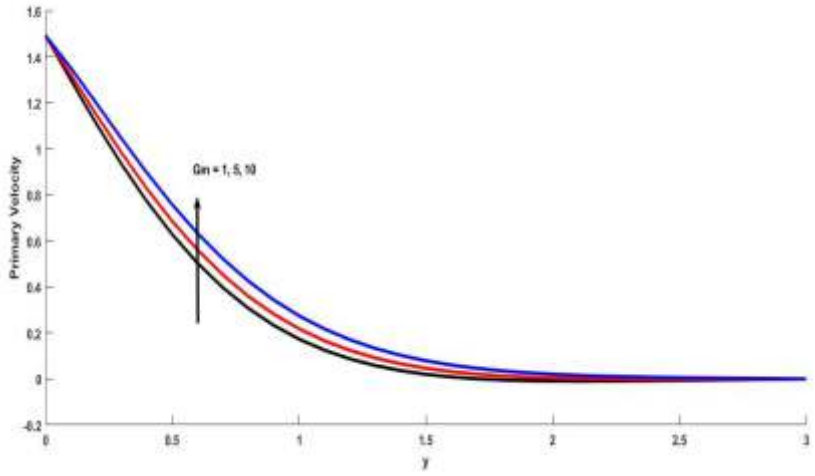

Fig. 14: Primary velocity u for different values of y and Gm.

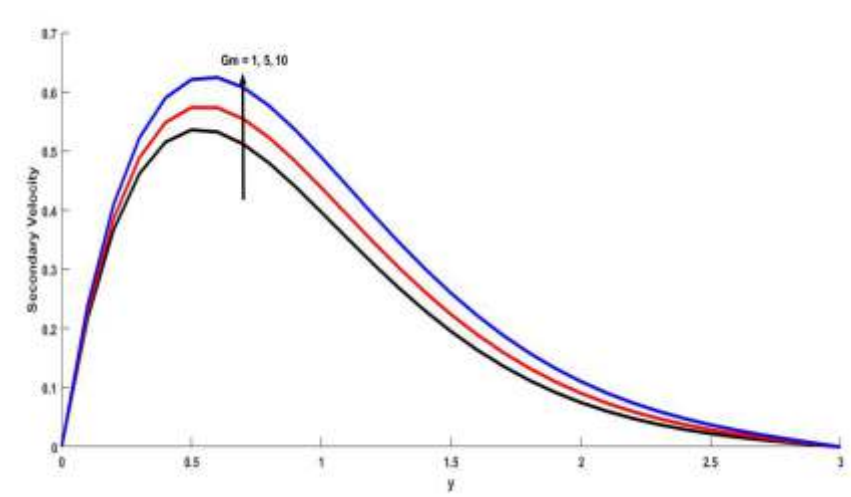

Fig. 15: Primary velocity u for different values of y and Gm.

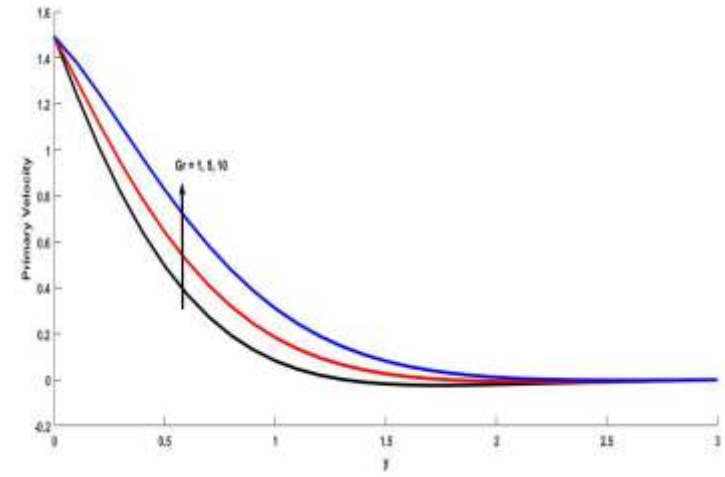

Fig. 16: Primary velocity u for different values of y and Gr.

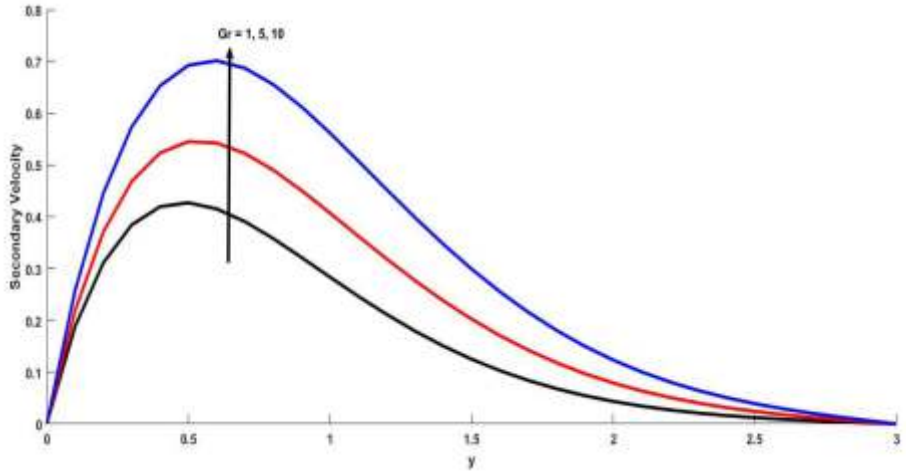

Fig.17: Primary velocity u for different values of y and Gr.

Figs. 2 and 3 show that, as Hall current m tends to accelerated flow in both directions. What happens to the main and secondary fluid velocities as a function of the Casson fluid parameter is depicted in Figures 4 and 5. It is found that the primary velocity drops as the Casson fluid parameter rises across the boundary layer region , while the secondary velocity rises at high values and subsequently falls as the value rises. The yield stress drops as a result of a rise in the Casson parameter, velocity boundary layer reduces. Because of the effect of the fluid's flexibility, Casson fluid has a tendency to slow down the motion in the x'-direction. Figs. 6 and 7 show how the effects of magnetic parameter M on primary and secondary fluid velocities, respectively. Both velocities will decrease as the magnitude of M increases. This is the cause of the observed behavior. The velocities profiles have been presented in Figures 8 and 9 with different values of permeability parameter, while the other parameters have been kept constant. It has been observed that the permeability of porous medium is a par ameter that has a tendency to promote fluid flow motion in both directions.

The effects of K on the fundamental and auxiliary fluid velocities which is seen in Figures 10 and 11. From the figures, it is concluded that the main velocity drops with rising K, while the secondary flow accelerated with K. As a result, the rotation parameter K tends to slow fluid flow in the principal flow directions while speeding it up in the secondary flow directions. This makes sense because the rotational Coriolis force causes a reversal of the primary flow direction of a fluid, causing a secondary flow. The chemical reaction and Soret effects on the concentration profile is depicted in Figures 12 and 13. Thermo-diffusion tends to enhance mass transfer, while chemical reaction tends to lower concentrations everywhere in the flow field. Figures 14-17 shows the Gm and Gr effects on primary and secondary velocities respectively. As a result of the picture, one can draw the conclusion that Gm and Gr have a tendency to accelerate in both directions.

CONCLUSION OF THE WORKS

The concluding summed up are as follows:

- All parameters have the same impact whether the wall temperature is raised or kept constant.
- The Primary and secondary velocities were boosted by both Grashof numbers. Permeability parameter appears to have the same behaviour.
- Magnetic fields tend to reduce the motion in both directions.
- Both the Casson parameter and the rotation number have the effect of slowing down the velocities.
- The concentration profile is delayed due to chemical reactions. Impacts on the concentration profile were boosted up by a Soret number.

Appendix:

$a_0 = \frac{M^2(1-im)}{1+m^2} + \frac{1}{k_1} - 2ik^2$	$a_1 = 1 + \frac{1}{\gamma}$	$a_2 = \frac{Pr}{Sc} - 1$
$a_3 = \frac{K_r}{a_2}$	$a_4 = \frac{-S_r\, P_r}{a_2}$	$a_5 = a_1\, P_r - 1$
$a_6 = \frac{a_0}{a_5}$	$a_7 = \frac{-Gr}{a_5}$	$a_8 = a_1\, S_c - 1$
$a_9 = a_1\, S_c\, K_r - a_0$	$a_{10} = \frac{a_9}{a_8}$	$a_{11} = \frac{-Gm}{a_8}$
$a_{12} = a_1\, P_r - 1$	$a_{13} = \frac{a_0}{a_{12}}$	$a_{14} = \frac{-G_m\, a_5}{a_{12}}$
$A = a_{15} = \frac{-a_7}{a_6}$	$a_{16} = \frac{a_{11}}{a_{10}}$	$a_{17} = \frac{a_{11}}{a_{10^2}}$
$a_{18} = \frac{a_{11}}{1+a_{10}} - a_{16} - \frac{a_{17}}{1+a_{10}}$	$a_{19} = \frac{a_{11}\, a_4}{a_3 + a_{10}}$	$a_{20} = \frac{-a_{11} a_4}{a_3 + a_{10}}$

$a_{21} = \frac{a_{14}}{a_3 - a_{13}}$	$a_{22} = \frac{a_{14}}{a_{13} - a_3}$	$a_{23} = -a_{15} - a_{18}$ $a_{24} = a_{20} - a_{17}$ $a_{25} = a_{19} - a_{21}$

REFERENCES:

[1] J. Hartmann and F. Lazarus, "Kgl. Danske Videnskab. Selskab, Mat," *Fys. Medd*, vol. 15, no. 6, p. 7, 1937.

[2] J. A. Shercliff, "Textbook of magnetohydrodynamics," 1965.

[3] E. H. Hall, "On a new action of the magnet on electric currents," *Am. J. Math.*, vol. 2, no. 3, pp. 287–292, 1879.

[4] E. M. Aboeldahab and E. M. E. Elbarbary, "Hall current e € ect on magnetohydrodynamic free-convection ¯ ow past a semi-in ® nite vertical plate with mass transfer," vol. 39, pp. 1641–1652, 2001.

[5] P. K. Sharma, "Fluctuating thermal and mass diffusion on unsteady free convection flow past a vertical plate in slip-flow regime," *Lat. Am. Appl. Res.*, vol. 35, no. 4, pp. 313–319, 2005.

[6] O. D. Makinde, "Free convection flow with thermal radiation and mass transfer past a moving vertical porous plate B," vol. 32, pp. 1411–1419, 2005, doi: 10.1016/j.icheatmasstransfer.2005.07.005.

[7] S. Mukhopadhyay, P. R. De, K. Bhattacharyya, and G. C. Layek, "Casson fluid flow over an unsteady stretching surface," *Ain Shams Eng. J.*, vol. 4, no. 4, pp. 933–938, 2013, doi: 10.1016/j.asej.2013.04.004.

[8] D. Sarma and K. K. Pandit, "Effects of Hall current , rotation and Soret effects on MHD free convection heat and mass transfer flow past an accelerated vertical plate through a porous medium," *Ain Shams Eng. J.*, vol. 9, no. 4, pp. 631–646, 2018, doi: 10.1016/j.asej.2016.03.005.

[9] C. S. M. Poornima, "Unsteady MHD Casson fluid flow through vertical plate in the presence of Hall current," *SN Appl. Sci.*, vol. 1, no. 12, pp. 1–14, 2019, doi: 10.1007/s42452-019-1656-0.

[10] Patel, H. R. (2019). Effects of cross diffusion and heat generation on mixed convective MHD flow of Casson fluid through porous medium with non-linear thermal radiation. Heliyon, 5(4), e01555.

[11] Prasad, D. K., Chaitanya, G. K., & Raju, R. S. (2019). Double diffusive effects on mixed convection Casson fluid flow past a wavy inclined plate in presence of Darcian porous medium. Results in Engineering, 3, 100019.

[12] Krishna, M. V., Sravanthi, C. S., & Gorla, R. S. R. (2020). Hall and ion slip effects on MHD rotating flow of ciliary propulsion of microscopic organism through porous media. International Communications in Heat and Mass Transfer, 112, 104500.

[13] Krishna, M. V., Ahamad, N. A., & Chamkha, A. J. (2021). Radiation absorption on MHD convective flow of nanofluids through vertically travelling absorbent plate. Ain Shams Engineering Journal, 12(3), 3043-3056.

[14] Li, Y. X., Rehman, M. I. U., Huang, W. H., Khan, M. I., Khan, S. U., Chinram, R., & Kadry, S. (2022). Dynamics of Casson nanoparticles with non-uniform heat source/sink: A numerical analysis. Ain Shams Engineering Journal, 13(1), 101496.

[15] Reddy, B. P., Makinde, O. D., & Hugo, A. (2022). A computational study on diffusion-thermo and rotation effects on heat generated mixed convection flow of MHD Casson fluid past an oscillating porous plate. International Communications in Heat and Mass Transfer, 138, 106389.

[16] Patel, H. R., & Patel, S. D. (2022). Heat and mass transfer in mixed convection MHD micropolar fluid flow due to non-linear stretched sheet in porous medium with non-uniform heat generation and absorption. Waves in Random and Complex Media, 1-31.

[17] Patel, H. R., Patel, S. D., & Darji, R. (2022). Mathematical Study of unsteady micropolar fluid flow due to non-linear stretched sheet in the presence of magnetic field. International Journal of Thermofluids, 16, 100232.

[18] M.P. Mkhatshwa and M. Khumalo, Double diffusion and Hall effects on

MHD sinusoidal natural convection flow of silver water-based nanofluid from a porous vertical plate, Partial Differential Equations in Applied Mathematics (2023)

[19] Sahoo, A., & Nandkeolyar, R. (2023). Entropy generation in magnetohydrodynamic radiative non-Darcy slip flow of a Casson nanofluid with Hall effects and activation energy. Journal of Magnetism and Magnetic Materials, 170712.

[20] G. K. Batchelor, An Introduction to Fluid Dynamics. London: Cambridge University Press; 1987.